

1 **Growth limiting factors and climate response variability in Norway spruce**  
2 **(*Picea abies* L.) along an elevation and precipitation gradients in Slovenia**

3

4 Jernej Jevšenak<sup>1, \*</sup>, Ivan Tychkov<sup>2</sup>, Jožica Gričar<sup>1</sup>, Tom Levanič<sup>1</sup>, Jan Tumajer<sup>3, 4</sup>, Peter  
5 Prislan<sup>5</sup>, Domen Arnič<sup>5</sup>, Margarita Popkova<sup>2</sup>, Vladimir V. Shishov<sup>2</sup>

6

7 <sup>1</sup>Department of Forest Yield and Silviculture, Slovenian Forestry Institute, Večna pot 2, 1000  
8 Ljubljana, Slovenia

9 <sup>2</sup>Laboratory for integral studies of forest dynamics of Eurasia, Siberian Federal University,  
10 Akademgorodok st., 50/2, Krasnoyarsk, 660075, Russia

11 <sup>3</sup>Department of Botany and Landscape Ecology, University of Greifswald, Soldmannstraße  
12 15, 17487 Greifswald, Germany

13 <sup>4</sup>Department of Physical Geography and Geoecology, Faculty of Science, Charles University,  
14 Albertov 6, 12843 Prague, Czech Republic

15 <sup>5</sup>Department of Forest Technique and Economics, Slovenian Forestry Institute, Večna pot 2,  
16 1000 Ljubljana, Slovenia

17 **E-mail address of the corresponding author:** [jernejevsenak@gozdis.si](mailto:jernejevsenak@gozdis.si)

18 **The final version of the manuscript:** <https://doi.org/10.1007/s00484-020-02033-5>)

19 **Please cite this article as:** Jevšenak, J., Tychkov, I., Gričar, J., Levanič, T., Tumajer, J., Prislan,  
20 P., Arnič, D., Popkova, M., Shishov, V.V., 2020. Growth-limiting factors and climate response  
21 variability in Norway spruce (*Picea abies* L.) along an elevation and precipitation gradients in  
22 Slovenia. International Journal of Biometeorology. [https://doi.org/10.1007/s00484-020-](https://doi.org/10.1007/s00484-020-02033-5)  
23 [02033-5](https://doi.org/10.1007/s00484-020-02033-5)

24 **Abstract:**

25 Norway spruce (*Picea abies* L.) is among the most sensitive coniferous species to ongoing  
26 climate change. However, previous studies on its growth response to increasing temperatures  
27 have yielded contrasting results (from stimulation to suppression), suggesting highly site-  
28 specific responses. Here, we present the first study that applies two independent approaches,  
29 i.e. the non-linear, process-based Vaganov-Shashkin (VS) model and linear daily response  
30 functions. Data were collected at twelve sites in Slovenia differing in climate regimes and  
31 ranging elevation between 170 and 1300 m a.s.l. VS model results revealed that drier Norway  
32 spruce sites at lower elevations are mostly moisture limited, while moist high-elevation sites  
33 are generally more temperature limited. Daily response functions match well the pattern of  
34 growth limiting factors from the VS model and further explain the effect of climate on radial  
35 growth: prevailing growth limiting factors correspond to the climate variable with higher  
36 correlations. Radial growth correlates negatively with rising summer temperature and  
37 positively with higher spring precipitation. The opposite response was observed for the  
38 wettest site at the highest elevation, which positively reacts to increased summer  
39 temperature and will most likely benefit from a warming climate. For all other sites, the future  
40 radial growth of Norway spruce largely depends on the balance between spring precipitation  
41 and summer temperature.

42

43 **Keywords:** Vaganov-Shashkin model; climate-growth correlations; tree rings; process-based  
44 modelling; dendroTools; dendroclimatology

45

46

47 **1. INTRODUCTION**

48 Norway spruce (*Picea abies* L.) is among the most important European tree species from both  
49 an economic and ecological point of view (Caudullo et al. 2016; Brus et al. 2012). In previous  
50 centuries, it was preferred for planting in managed forests due to its fast growth, high quality  
51 wood, wide ecological amplitude and adaptive capacity to various site conditions (Klimo et al.  
52 2000; Spiecker 2003). In recent decades, however, Norway spruce has suffered from natural  
53 hazards such as windthrows, ice-storms, insect outbreaks and droughts (Schelhaas et al. 2003;  
54 Seidl et al. 2016), resulting in a decline in its share in the national growing stocks of many  
55 European countries, including Austria (BMLFUW 2017), the Czech Republic (MZe 2018),  
56 Germany (BMEL 2015), Latvia (Tērauds et al. 2011), Slovakia (MPSR 2019), Slovenia (Skudnik  
57 et al. 2019) and southern Sweden (Valinger et al. 2014). Furthermore, some projections show  
58 that this trend will continue for the whole of Europe in the future (Buras and Menzel 2019;  
59 Hanewinkel et al. 2013). Extreme climate conditions, increasing temperatures and altered  
60 precipitation patterns are among the highest risks related to less suitable habitat conditions  
61 for Norway spruce in future decades (Lévesque et al. 2013; van der Maaten-Theunissen et al.  
62 2013). Despite the evident threats associated with a warmer and drier climate, there is  
63 evidence that Norway spruce is exhibiting faster growth than that recorded in the past  
64 century, especially at higher elevations close to the timberline (Pretzsch et al. 2014; Cienciala  
65 et al. 2018; Kahle et al. 2008; Ponocná et al. 2016; Hartl-Meier et al. 2014). Norway spruce  
66 has shown contrasting responses to climate at lower and higher elevations (Andreassen et al.  
67 2006; Kolář et al. 2017; Sidor et al. 2015), indicating that site-specific conditions need to be  
68 considered to more accurately estimate its future growth, vitality and habitat suitability  
69 (Reyer et al. 2017).

70 Although Norway spruce is among the most studied European species, predictions of its  
71 response to diverse growth conditions (environmental changes) remain challenging. Models  
72 based on realistic underlying processes would improve our understanding of the performance  
73 of the species in the future. Furthermore, silvicultural practices could be more effectively  
74 adjusted in order to mitigate the effects of climate change (Klopčič et al. 2017). Process-based  
75 modelling provides a unique insight into underlying processes resulting in tree growth (Guiot  
76 et al. 2014). One frequently applied process-based model for simulations of intra- and inter-  
77 annual tree-ring characteristics of conifers is the Vaganov-Shashkin (VS) model (Vaganov et  
78 al. 2006; Shishov et al. 2016), which incorporates the nonlinear and nonstationary  
79 relationship between climate and radial tree growth. The VS model incorporates the principle  
80 of growth limiting factors through the calculation of growth potential on a daily basis as a  
81 result of soil moisture, temperature and solar irradiance. The most limiting factor defines the  
82 potential for growth for each day. With the parameterization process, the effect of climate  
83 on radial conifer growth is defined and available for interpretation. To the best of our  
84 knowledge, the VS model has not yet been applied to Norway spruce, although Tumajer et al.  
85 (2017) studied moisture and temperature limitations in Norway spruce in the Czech Republic  
86 with the VS-Lite model (Tolwinski-Ward et al. 2011), which is a simplified VS model based on  
87 monthly climatic data.

88 To better understand the underlying growth limiting factors of Norway spruce and how they  
89 vary with respect to different site conditions, we analysed spruce chronologies from twelve  
90 sites in Slovenia. Slovenia is characterized by a transitional climate with wide local climatic  
91 variability and pronounced gradients that support the growth of this species on a wide variety  
92 of sites. Thus, the findings of our study could be applied to different sites across Europe with  
93 similar growth conditions. The main objectives of our study were 1) to parameterise the VS  
94 model for the selected Norway spruce sites, 2) to extract daily growth rates and infer about

95 limiting growth factors and how they vary in time, 3) to further use daily growth rates to infer  
96 about growing season patterns and 4) to analyse climate-growth correlations with daily  
97 response function and compare the results with the VS model. We hypothesise that specific  
98 sites will show variable growth patterns and responses to climatic conditions, i.e. growth  
99 stimulation/reduction due to increasing temperature in moist/dry sites.

100

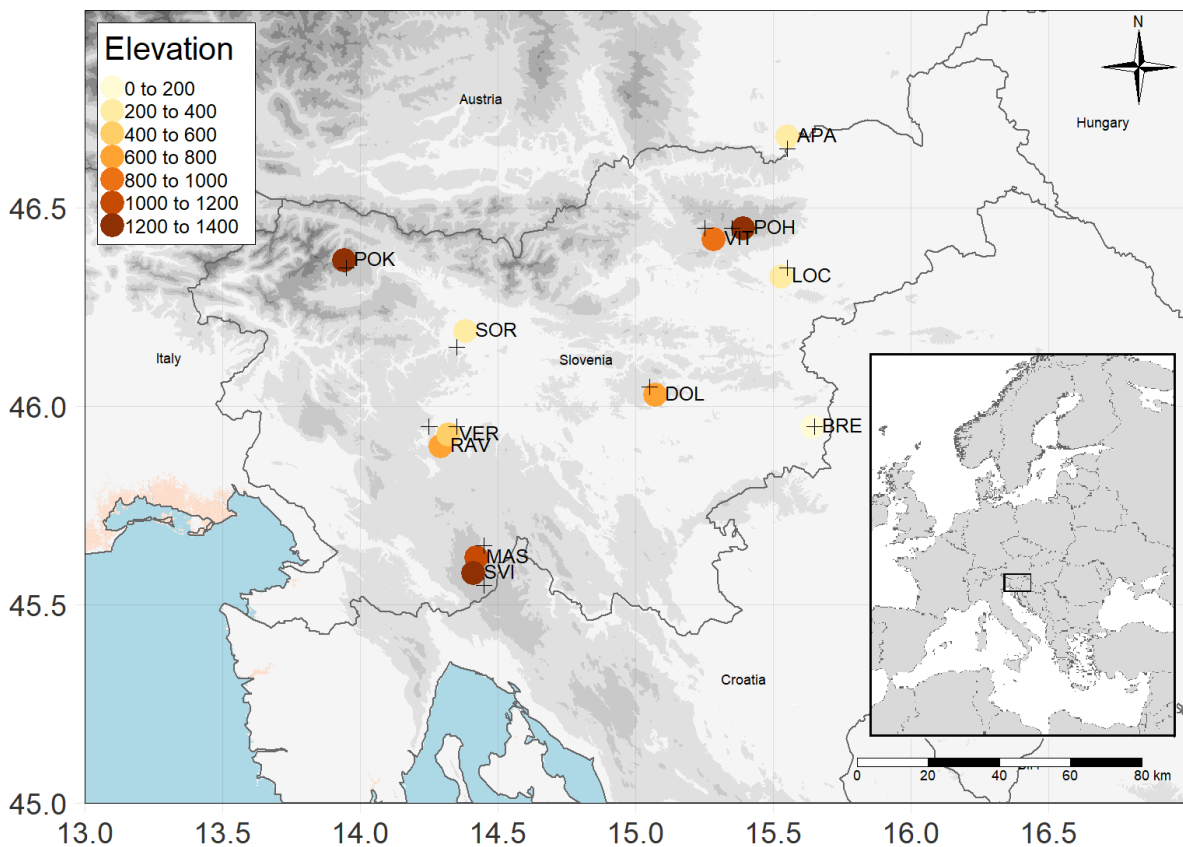
## 101 **2. METHODS**

### 102 **2.1 Site description and climate data**

103 Twelve spruce sites were selected for sampling in 2016–2018. The sites ranged from dry and  
104 warm low elevation sites in eastern Slovenia to moist and cold high elevation sites in the  
105 central, north-western and southern parts of the country (Figure 1). All sampled sites are  
106 managed forests in the adult developmental stage, with Norway spruce as the dominant tree  
107 species. The main differences between the selected sites are elevation, climate regimes and  
108 soil types (Table 1). For each site, daily precipitation sums and mean temperature data were  
109 extracted for the closest grid point from the E-OBS gridded climate datasets (Cornes et al.  
110 2018). E-OBS version 21.0e on a 0.1-degree regular grid was used, which starts on January 1,  
111 1950. To account for differences in longitudes, latitudes and elevations between E-OBS grid  
112 points and site locations, climate data was spatially interpolated using cokriging, where  
113 elevation was used as covariate for the cokriging method (Apaydin et al. 2004; Adhikary et al.  
114 2017).

115 **Table 1:** Site descriptions with annual mean temperature (T) and precipitation (P) sums in  
 116 the period 1950–2018.

Site	Short	Lon	Lat	Elevation [m]	Annual T [°C]	Annual P [mm]	Soil type
Apače	APA	15.55	45.68	210	9.3	979	Dystric Fluvisol
Brežice	BRE	15.64	45.95	170	10.6	1011	Eutric Cambisol
Dole	DOL	15.07	46.03	640	9.1	1194	Chromic Cambisol
Loče	LOC	15.53	46.33	310	9.8	1069	Eutric Cambisol
Masun	MAS	14.42	45.62	1000	6.4	1605	Chromic Cambisol
Pohorje	POH	15.39	46.45	1285	6.8	1166	Dystric Cambisol
Pokljuka	POK	13.94	46.37	1300	5.3	1852	Rendzic Leptosol
Ravnik	RAV	14.29	45.90	750	9.2	1641	Rendzic Leptosol
Sorško Plain	SOR	14.38	46.19	370	9.4	1464	Eutric Cambisol
Sviščaki	SVI	14.41	45.58	1200	6.3	1652	Rendzic Leptosol
Verd	VER	14.32	45.93	595	9.6	1587	Rendzic Leptosol
Vitanje	VIT	15.28	46.42	940	6.9	1181	Dystric Cambisol



118

119 **Figure 1:** Site locations (coloured dots) with elevation in meters and the closest grid points  
 120 (crosses) from the E-OBS daily dataset.

121

## 122 2.2 Dendrochronological analysis

123 At each site, at least 20 dominant or codominant adult trees were cored from the opposite  
 124 sides using a Pressler borer. Tree cores were dried in the laboratory, fixed in wooden holders  
 125 and sanded to obtain a smooth surface with clearly visible borders between the tree rings.  
 126 High resolution images were taken with the ATRICS (Levanič 2007). Tree-ring widths were  
 127 then measured in CooRecorder & CDendro software (Cybis), and the final cross-dating was  
 128 done in PAST-5 (SCIEM). A few series showed low correlations with site chronologies and were  
 129 therefore not used in further analysis. All series were standardised using the *detrend()*  
 130 function from the dplR R package (Bunn 2008). A modified negative exponential function was  
 131 fitted to the raw tree-ring width series and to obtain final tree-ring indices (TRWi), measured

132 values were divided by fitted ones. To build site chronologies, TRWi were pre-whitened and  
 133 averaged using a robust biweight mean. The basic parameters of the site chronologies are  
 134 given in Table 2.

135

136 **Table 2:** Descriptive statistics for site chronologies with number of trees (and cores), mean  
 137 chronology length, earliest and recent year, and mean *Pearson* correlation among detrended  
 138 series (*rbar*).

Site	N	Length	First year	Last year	rbar
APA	20 (40)	95	1889	2018	0.44
BRE	20 (39)	76	1910	2017	0.42
DOL	19 (38)	100	1879	2018	0.37
LOC	19 (35)	108	1883	2017	0.42
MAS	21 (42)	110	1863	2016	0.29
POH	20 (40)	124	1882	2016	0.38
POK	21 (41)	136	1867	2016	0.33
RAV	20 (39)	97	1870	2016	0.37
SOR	20 (39)	98	1862	2016	0.40
SVI	20 (39)	141	1821	2016	0.46
VER	21 (41)	111	1800	2017	0.38
VIT	22 (43)	132	1839	2017	0.45

139

### 140 **2.3 Vaganov-Shashkin (VS) process-based model**

141 The VS model simulates the kinetics of radial growth of conifers, more specifically the  
 142 characteristics of a representative radial file of tracheids, such as their number, lumens and  
 143 cell-wall thicknesses (Guiot et al. 2014). It has been successfully tested in various biomes, e.g.  
 144 near the polar forest limit, in the taiga and steppe, in semiarid and monsoon climates



145 (Vaganov et al. 2006), in a Mediterranean climate (Touchan et al. 2012), in a humid  
146 continental climate (St. George et al. 2008), in the cold and dry continental climate of north-  
147 western China (He et al. 2018; He et al. 2017b; He et al. 2017a) and in the continental climate  
148 of Siberia (Shishov et al. 2016; Tychkov et al. 2019).

149 The radial profile is the result of the simulation of cambium activity, where cells divide and  
150 grow depending on daily weather conditions (Vaganov et al. 2006). The characteristics of the  
151 radial files can also be summarized into annual characteristics to obtain estimates for tree-  
152 ring parameters such as width and density. For the VS parameterization (see below) and  
153 simulation purposes, we used VS-oscilloscope (Shishov et al. 2016), while there is also a  
154 MATLAB version available (Anchukaitis et al. 2020). VS-oscilloscope is an interactive visual  
155 tool of the VS model that enables the selection of an optimal combination of model  
156 parameters while simultaneously comparing the observed and modelled TRWi. Input  
157 variables for the VS model are daily temperature and precipitation, while daily solar  
158 irradiation is calculated from latitude and day of the year. Precipitation is used to estimate  
159 soil moisture. This model incorporates the principle of growth limiting factor, which defines  
160 the growth rate for each day. In the first step, the VS model calculates the partial daily growth  
161 rates  $Gr(t)$  for temperature, soil moisture and solar irradiance. In the second step, the  
162 minimum from daily temperature and soil moisture growth rates is multiplied by the solar  
163 irradiance growth rate to obtain  $G(t)$  (Evans et al. 2006). The resulting integral daily growth  
164 rate expresses the potential for radial growth on each day and varies between 0 and 1. Values  
165 close to 0 indicate dormancy or climatically unfavourable days of the growing season, usually  
166 in winter or during summer drought periods, while values close to 1 indicate favourable  
167 climate conditions for radial growth, such as warm summer days with both daily temperature  
168 and moisture in optimal intervals.

## 169 **2.4 VS model parameterization and evaluation**

170 All chronologies were split into a period for model parameterization (calibration), i.e. 1980–  
171 2016 (or the most recent year), and a period for model evaluation (verification), i.e. 1950–  
172 1979. To evaluate the accuracy of VS model simulations, the *Pearson* correlation coefficient  
173 ( $r$ ), root-mean-square error (RMSE), mean bias and Gleichläufigkeit statistics (Buras and  
174 Wilmking 2015; Eckstein and Bauch 1969) were calculated between simulated and observed  
175 TRWi. In addition, to account for differences in simulated and observed variability, a simple  
176 variance ratio was calculated as the quotient between simulated and observed variance.

177 Partial daily growth rates were further used to analyse growth limiting factors for each site  
178 and how they vary in time. In addition, trends in growing season timing since 1950, namely  
179 the date of the onset and end of the growing season, were analysed and used to infer about  
180 temporal changes in cambial phenology. The onset of the growing season was defined as the  
181 first day in the year when the cumulative temperature sum exceeds the minimum  
182 temperature threshold for growth, while the end of growing season was defined as the day  
183 in the year when the cumulative temperature sum falls below the temperature threshold for  
184 growth and growth rate is less than the critical value. See more information about the final  
185 parameter values in Supplementary Table 1.

186

## 187 **2.5 Daily response functions**

188 To further supplement the VS model simulations, daily correlations were calculated between  
189 TRWi and climate data using the dendroTools R package (Jevšenak and Levanič 2018; Jevšenak  
190 2020). The function *daily\_response\_seascore()* was applied, which uses a moving window of  
191 variable widths and calculates partial correlation coefficients between an aggregated climate  
192 variable and selected tree-ring proxy, while simultaneously controlling for the second climate

193 variable. The function was applied to both climate variables: temperature, while considering  
194 precipitation as a control, and vice versa. To calculate daily correlations, all window widths  
195 between 21 and 270 consecutive days were considered, and partial correlations were  
196 calculated using a bootstrap procedure with 1000 replicates. Such calculations provide robust  
197 correlation estimates but are also computationally expensive.

198

### 199 3. RESULTS

200 The VS model was parameterised for each of the twelve Norway spruce sites in Slovenia, and  
201 the final parameter values are presented in Supplementary Table 1. VS parameters related to  
202 temperature thresholds correlated negatively with site elevations, while parameters related  
203 to soil moisture thresholds generally showed less significant and positive correlations with  
204 elevation (Supplementary Figure 1). Warmer low elevation sites had a higher minimum  
205 threshold temperature (7 °C) and higher temperature sums (80 °C) for trees to start growing  
206 season, while for high elevation and colder sites, e.g. the coldest site SVI, the minimum  
207 temperature to start growth was 4 °C and the temperature sum was 69 °C.

208 VS simulations provided significant correlations between modelled and actual TRWi for all  
209 analysed sites (Figure 2, Table 3). On average, the correlation coefficient was 0.598 ( $p < 10^{-4}$ )  
210 for the calibration period and 0.508 ( $p < 10^{-2}$ ) for the verification period. The best results were  
211 obtained for low-elevation site BRE, where correlations for calibration and verification  
212 periods were both above 0.75 ( $p < 10^{-5}$ ). The lowest verification results were obtained for site  
213 SVI, where correlations for calibration and verification were around 0.34 ( $p < 0.05$ ).



214

215 **Figure 2:** Simulated (blue lines) and observed (red lines) TRWi chronologies for the calibration  
 216 (1980–2018) and verification (1950–1979) periods. Chronologies are sorted based on a  
 217 precipitation gradient from drier sites (upper panels) to wetter sites (lower panels).

218 **Table 3:** Evaluation results for the comparison between simulated and observed TRWi  
 219 chronologies for the calibration and verification period: Pearson correlation coefficient (r),  
 220 root-mean-square error (RMSE), mean bias, Gleichläufigkeit (GLK%) and variance ratio (VR).

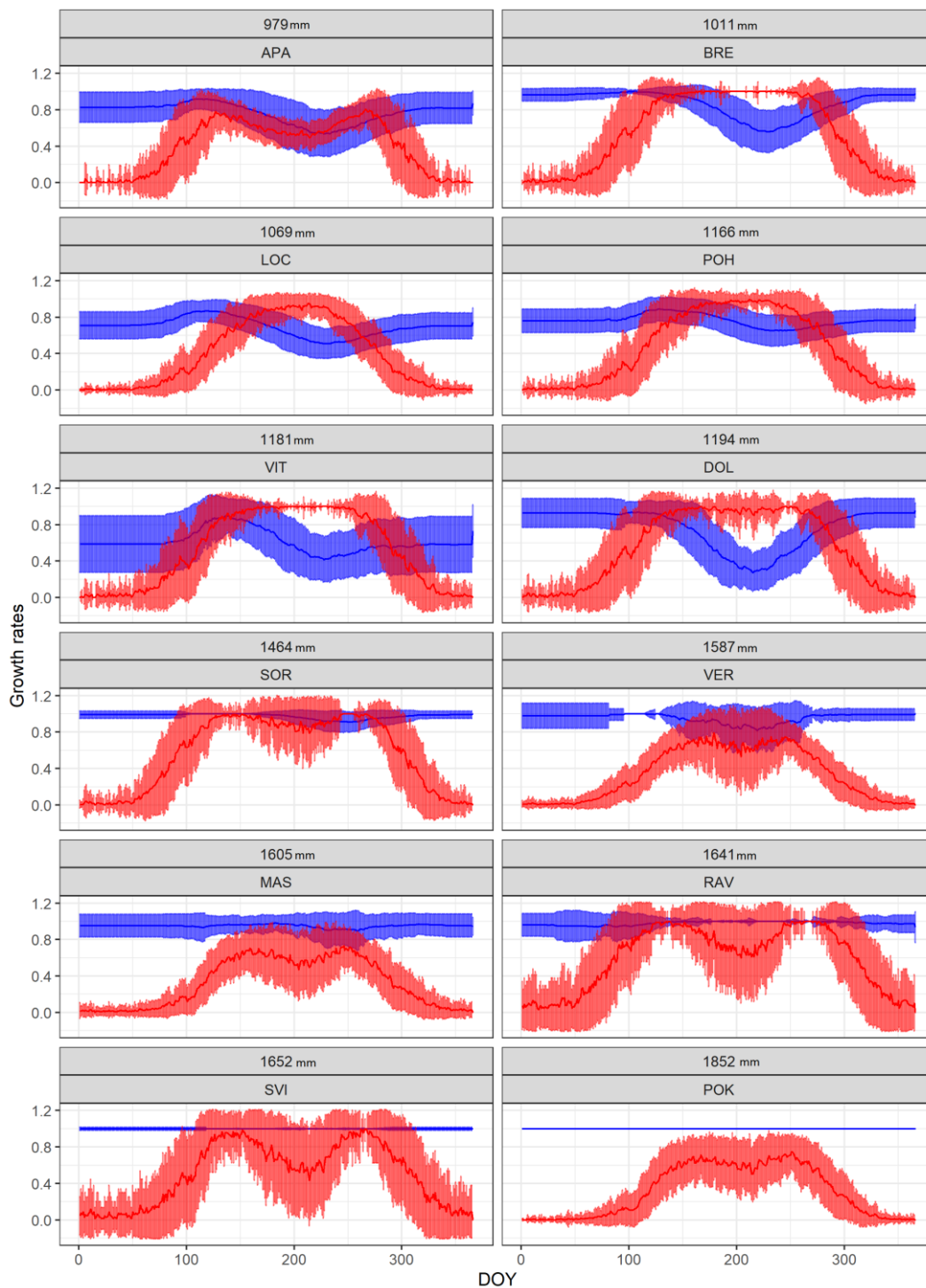
Site	Period	Years	r	RMSE	bias	GLK%	VR <sub>1</sub>
BRE	Calibration	1980 – 2017	0.77	0.14	0.00	0.73	0.40 <sup>222</sup>
BRE	Verification	1950 – 1979	0.75	0.10	0.00	0.76	0.81
LOC	Calibration	1980 – 2017	0.59	0.16	-0.01	0.73	0.54 <sup>223</sup>
LOC	Verification	1950 – 1979	0.56	0.11	0.00	0.66	1.03
APA	Calibration	1980 – 2018	0.54	0.22	-0.02	0.71	0.25 <sup>224</sup>
APA	Verification	1950 – 1979	0.37	0.15	0.02	0.62	0.85 <sup>225</sup>
VIT	Calibration	1980 – 2017	0.64	0.16	-0.01	0.73	0.73
VIT	Verification	1950 – 1979	0.45	0.16	-0.01	0.55	1.68 <sup>226</sup>
DOL	Calibration	1980 – 2018	0.56	0.17	0.02	0.66	0.61 <sup>227</sup>
DOL	Verification	1950 – 1979	0.41	0.15	-0.02	0.52	1.52
POH	Calibration	1980 – 2016	0.42	0.17	-0.01	0.58	0.41 <sup>228</sup>
POH	Verification	1950 – 1979	0.45	0.12	0.01	0.52	1.24
SOR	Calibration	1980 – 2016	0.78	0.17	-0.01	0.86	0.11 <sup>229</sup>
SOR	Verification	1950 – 1979	0.54	0.11	0.01	0.62	0.21 <sup>230</sup>
VER	Calibration	1980 – 2017	0.67	0.09	0.01	0.76	0.58
VER	Verification	1950 – 1979	0.72	0.12	-0.04	0.83	0.28 <sup>231</sup>
MAS	Calibration	1980 – 2016	0.57	0.10	0.01	0.75	0.62 <sup>232</sup>
MAS	Verification	1950 – 1979	0.42	0.09	0.00	0.59	1.31
RAV	Calibration	1980 – 2016	0.66	0.13	-0.01	0.81	0.26 <sup>233</sup>
RAV	Verification	1950 – 1979	0.62	0.13	0.03	0.66	0.22 <sup>234</sup>
SVI	Calibration	1980 – 2016	0.33	0.15	-0.01	0.64	0.92
SVI	Verification	1950 – 1979	0.35	0.14	0.01	0.69	1.39 <sup>235</sup>
POK	Calibration	1980 – 2016	0.64	0.11	-0.02	0.75	0.46
POK	Verification	1950 – 1979	0.45	0.09	0.01	0.72	1.03 <sup>236</sup>

238 Daily growth rates revealed different growth limiting patterns for the analysed sites (Figure  
239 3). To explain the differences in growth limitations among spruce sites, the annual  
240 precipitation pattern turned out to be more appropriate than elevation. At the beginning of  
241 growing seasons, all sites are temperature limited, while in late spring and summer seasons,  
242 sites that receive less than 1200 mm annually are mostly precipitation limited, while high  
243 elevation sites with more than 1600 mm of annual precipitation generally remain  
244 temperature limited. Some moderately wet sites (i.e. SOR, VER and RAV) showed mixed-  
245 precipitation and temperature signal. We observed a very moderate increase in temperature  
246 limitation for most of the higher elevation sites, while the temporal changes in moisture  
247 limitation are non-significant (Supplementary Figure 2). Those results indicate that temporal  
248 changes in growing season limiting factors for Norway spruce in Slovenia are only minor and  
249 mostly nonsignificant.

250 The temporal changes in onset and end of growing season were estimated from daily growth  
251 rates (Figure 4). The calculated trends indicated earlier onset and later end of the growing  
252 season for recent years, resulting in a longer growing season for the majority of the sites. A  
253 minor deviation from this pattern was observed for site MAS, which showed a slightly delayed  
254 onset of the growing season for recent years, while site BRE indicated earlier end of growing  
255 season. The estimated increase of the growing season duration ranged from 5.6 (SOR) to 1.0  
256 (BRE) days per decade. We did not observe any systematic pattern of growing season  
257 prolongation related to elevation, climate regimes or prevailing growth limiting factors.

258 Daily response functions revealed a consistent pattern of climate signal in TRWi: Higher  
259 precipitation sums had a positive effect and higher mean temperature had a negative effect  
260 on radial tree growth (Figure 5). The only clear exception was the wettest site POK, which  
261 showed almost no significant correlations with precipitation and the positive influence of

262 higher temperature. No significant precipitation correlation was observed also for site SVI,  
 263 which receives a relatively high amount of annual precipitation.



264

265 **Figure 3:** Daily growth rates as predicted by the VS model for the analysed sites based on  
 266 precipitation (blue colour) and temperature (red colour). Shown values represent the average  
 267 and standard deviation of each day of the year (DOY) for the entire analysed period, i.e. 1950–  
 268 2016. Above site abbreviations, mean annual sums of precipitation in millimetres (mm) are  
 269 given for the period 1950–2017.

## 270 4. DISCUSSION

### 271 4.1 The effect of climate on radial tree growth

#### 272 4.1.1 Growth limiting factors

273 The VS model describes the effect of climate on radial tree growth by applying the principle  
274 of growth limiting factor through realistic mechanistic equations. Drier Norway spruce sites  
275 at lower elevations are mostly moisture limited, while moist high-elevation sites are generally  
276 more temperature limited. We observed an interesting pattern of constant soil moisture  
277 effect for both the wettest sites (SVI and POK), where partial growth rates for soil moisture  
278 limitation are always close to 1, indicating the optimal soil moisture conditions throughout  
279 the year. Such results are expected and in accordance with previous studies focused on the  
280 analysis of limiting growth factors of Norway spruce across environmental gradients (Rabbel  
281 et al. 2018).

282 To distinguish between precipitation and temperature limited sites, precipitation seems to be  
283 more appropriate than commonly used elevational gradients (Touchan et al. 2016). Below  
284 1200 mm of annual precipitation, spruce sites are mostly precipitation limited, while above  
285 1600 mm, temperature defines tree growth through most of the growing season. Moderately  
286 wet sites, i.e. with annual precipitation sums of 1200-1600 mm showed a mixed precipitation-  
287 temperature signal. However, the defined thresholds are only approximate, and there are  
288 other site factors, such as soil type, slope, exposition and seasonal precipitation distributions,  
289 that interact with climate and define tree growth. For example, sites SOR and VER received a  
290 similar amount of annual precipitation, 1464 and 1587 mm, respectively, but SOR is more  
291 moisture limited, while VER is more temperature limited.

292 The identified growth limiting factors for Norway spruce correspond to those reported by  
293 Tumajer et al. (2017), who analysed moisture and temperature limitations in Norway spruce



294 in the Czech Republic tree-ring network with the VS-Lite model (Tolwinski-Ward et al. 2011).  
295 They found a clear pattern of temperature limited sites at higher elevations (above 800 m)  
296 and moisture limited sites at lower elevations (below 500 m), while mid-elevation  
297 chronologies were mostly characterised as mixed signal chronologies. However, our studies  
298 differ in the identified temporal shifts; while Tumajer et al. (2017) reported increasing soil  
299 moisture limitation for most of the analysed chronologies, we observed insignificant changes  
300 for soil moisture limitation and minorly increased temperature limitation for higher elevation  
301 sites. The differences between the two studies might arise from different methodological  
302 approaches, i.e. VS model vs VS-Lite model, different sampling strategies (random in the  
303 Czech Republic vs dominant trees in Slovenia) and different strategies to analyse temporal  
304 shifts. The growth limiting factor shifts from our study correspond to the actual climate trends  
305 at the analysed sites (Supplementary Figure 3), where mean annual temperatures exhibit a  
306 moderate increasing trend and precipitation patterns show no significant changes.

307 To put our results into a wider context, the VS model has often recognized soil moisture to be  
308 the prevailing driver of tree growth in dry areas, such as the cold Tibetan Plateau (He et al.  
309 2017a), warm Mediterranean (Touchan et al. 2012) and Siberia (Tychkov et al. 2019; Popkova  
310 et al. 2018). Often, temperatures play an important role at the beginning of the growing  
311 season (Rossi et al. 2008), while during the growing season, the environmental signal may  
312 change, and water availability becomes the main factor affecting growth (e.g. St. George et  
313 al. 2008). Temperature defined the onset of the growing season for all Norway spruce sites  
314 analysed in our study. However, to understand global drivers of tree growth and how they  
315 relate to local climate conditions, additional studies are needed to reveal the underlying  
316 physical dependences between tree growth and limiting site factors (Carrer et al. 2012).

#### 318 4.1.2 Daily response functions

319 The results of daily response functions (Figure 5, Supplementary Table 2) correspond well  
320 with the pattern of growth limiting factors from the VS model (Figure 3). In general, prevailing  
321 growth limiting factors correspond to the climate variable with higher correlations, although  
322 both temperatures and precipitation are significant at most sites. Some more moisture  
323 limited sites (e.g. BRE, LOC, VIT and SOR) showed more significant correlations with  
324 aggregated precipitation data, while more temperature limited sites showed more significant  
325 correlations with aggregated temperature data (e.g. APA, DOL, and POK) (Supplementary  
326 Table 2). Importantly, how the VS model and dendroTools correspond is more obvious for  
327 sites with higher correlations and better VS model performance. The benefit of applying the  
328 response functions is the information related to the positive/negative effect of a particular  
329 climate variable, which is not obvious from observing the growth limitation patterns (Figure  
330 3). For the drier low-elevation sites APA, BRE and LOC, we observed positive spring and  
331 summer correlations with precipitation sums, while higher precipitation in autumn resulted  
332 in negative correlations and decreased ring widths. This shift in correlations corresponds to a  
333 shift in the growth limiting factor, where soil moisture becomes less limiting and temperature  
334 limitation prevails (Figure 3).

335 All previous studies that considered a sufficiently wide elevation gradient reported two  
336 different response types for Norway spruce: 1) positive summer temperature correlations and  
337 (less significant) negative precipitation correlations for higher elevations close to timberline  
338 and 2) negative summer temperature correlations and positive precipitation correlations for  
339 lower elevations, e.g. for all of Norway (Andreassen et al. 2006), the Giant Mountains in the  
340 Czech Republic (Kolář et al. 2017), the Alps (Hartl-Meier et al. 2014) and the Eastern  
341 Carpathians in Romania (Sidor et al. 2015). Similarly, the analysis of colder sites from the

342 upper timberline from East-Central Europe (Ponocná et al. 2016) and the far north to the  
343 Arctic timber line (Mäkinen et al. 2000) revealed positive summer correlations and a barely  
344 significant positive precipitation effect. Positive precipitation correlations and negative  
345 correlations for summer temperature are commonly reported for Norway spruce from mid to  
346 low elevations, e.g. for south-western (van der Maaten-Theunissen et al. 2013) and western  
347 (Rabbel et al. 2018) Germany, the Eastern Carpathians in Romania (Bouriaud and Popa 2009)  
348 and the lowlands of Poland (Koprowski and Zielski 2006).

349 The results of our response analysis are in accordance with previous studies: higher winter  
350 and spring precipitation amounts have a positive effect on tree growth, while higher summer  
351 temperature is related to negative correlations for all low- and mid-elevation sites. In  
352 contrast, Pokljuka (POK) – the wettest site from the highest elevation – shows the opposite  
353 pattern. Sites SOR and POK were used in a comparison study by Levanič et al. (2008) and  
354 exhibited the same climate-growth patterns as shown in our study.

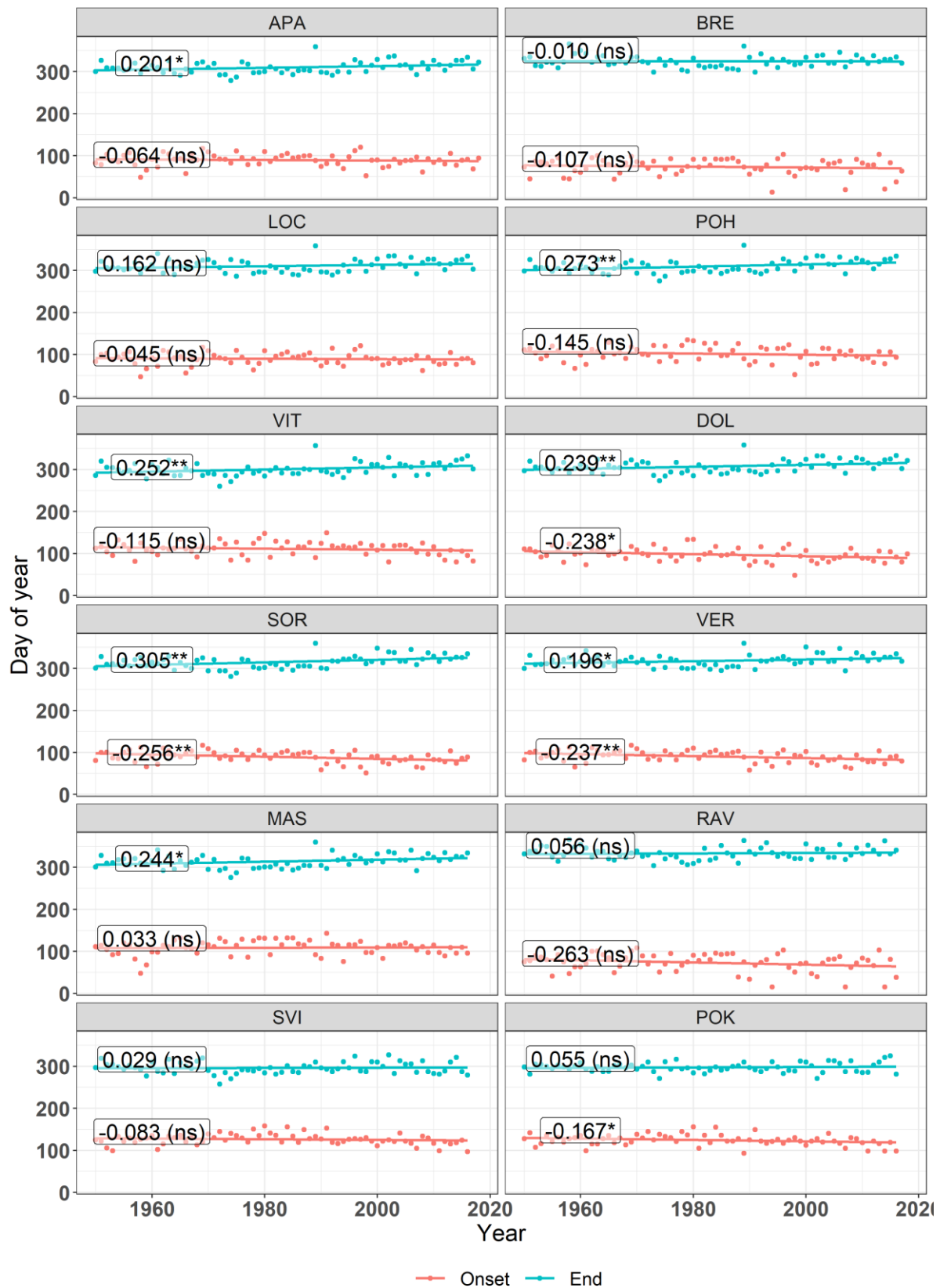
355 The shift between a positive and negative effect of temperature on the radial growth of  
356 spruce was reported to be somewhere between 13-13.5 °C (June temperature) (Sidor et al.  
357 2015; Andreassen et al. 2006), which corresponds well with the results from our study. We  
358 calculated the positive effect of higher temperatures for the Pokljuka (POK) site, where the  
359 mean June temperature (1950–2018) was 12.2 °C. Next the coldest (June) sites were SVI (13.5  
360 °C) and MAS (13.6 °C) which already exhibited a negative effect of higher temperatures.

361

#### 362 **4.2 Simulated growing season patterns**

363 The changes in growing season phenology were inferred from daily growth rates, which  
364 indicate the onset and end of the growing season (see Section 2.3 for definitions). The typical  
365 onset of the growing season was calculated to be on DOY 98, while the typical end of the

366 growing season was on DOY 311. Those estimates can be compared with direct observations  
367 by Gričar et al. (2014), who studied the xylogenesis at low- (400 m) and high-elevation (1200  
368 m) Norway spruce sites for three consecutive years (2009–2011). They reported the average  
369 onset DOY 103 (low elevation) and DOY 117 (high elevation), while the average end of the  
370 growing season was on DOY 241 (low elevation) and 228 (high elevation). Xylem formation  
371 phenology for sites SOR and POK were studied in 2002–2004 by Levanič et al. (2008), so we  
372 can directly compare the observed and simulated onset and end of the growing season  
373 (Supplementary Table 3). The agreement between the simulated and measured onset and  
374 end of the growing season was better for site POK, where the simulated onset was on average  
375 for 12 days earlier, while the simulated end was on average 48 days later than the measured.  
376 Therefore, there is a general agreement between the VS model simulations and xylogenesis  
377 observations, where the onset estimates are closer to field observations than those of the  
378 end of the growing season. Buttò et al. (2020) reported systematic overestimations in the  
379 predicted timing of tracheid differentiation phases by 1-20 days and concluded that the  
380 current formulation in the VS model is unable to explain the events in autumn. VS model  
381 currently lacks an appropriate module that would account for carbon storage processes which  
382 usually occur at the end of the growing season (Furze et al. 2019), when climate conditions  
383 are favourable. Ongoing efforts aim to improve the performance of the VS model by more  
384 properly accounting for carbon storage processes and subsequent carry-over effects in the  
385 subsequent spring. Although there are differences between the observed and simulated  
386 onset and end of the growing seasons, we assume that, in relative terms, temporal changes  
387 are systematic and VS simulations can be used to infer the cambial phenology trends and  
388 intra-annual variability.



389

390 **Figure 4:** Changes in the onset and end of the growing season as calculated from the daily  
 391 growth rates from the VS model. Labels depict slope parameters of calculated trends with the  
 392 following significance codes: \*\*\* ( $p < 0.001$ ), \*\* ( $p < 0.01$ ), \* ( $p < 0.05$ ) and ns  
 393 (nonsignificant).

394 Mainly due to a warming climate, changes in growing season patterns have already been  
395 reported around the globe based on observations of leaf phenology (Menzel and Fabian  
396 1999), satellite images (Park et al. 2016) and climatological records (Linderholm et al. 2008).  
397 Our analysis of growing season trends indicated the earlier onset and later end for recent  
398 years, which resulted in the prolongation of the growing season by 3.1 days per decade on  
399 average (Figure 4). A comprehensive overview of growing season changes is available by  
400 Linderholm (2006). Recently, Park et al. (2016) reported a prolongation of 2.60 days per  
401 decade (1984–2014) for the Northern Hemisphere based on an analysis of satellite  
402 observations. Our calculated trends based on VS simulations are within the intervals usually  
403 reported by others; therefore, we assume they realistically reflect growing season trends for  
404 the analysed sites.

405

### 406 **4.3 VS model performance**

407 The parameterization process resulted in realistic parameter values (Supplementary Table 1),  
408 which effectively reflected local site characteristics (Supplementary Figure 1). Temperature  
409 thresholds showed negative correlations with elevation, while precipitation thresholds  
410 showed less significant correlations with site characteristics. We assume that soil moisture  
411 parameters are much more related to local terrain characteristics and soil conditions and  
412 therefore show lower correlations. In general, low elevation sites had higher temperature  
413 thresholds to start growth, and sites with higher amounts of precipitation had a higher soil  
414 moisture threshold for the initiation of tree growth.

415 All correlations between modelled and actual tree-ring chronologies were significant ( $p <$   
416  $0.05$ ) for both calibration and verification data (Figure 2, Table 3). For the independent  
417 verification data, correlations ranged from 0.75 to 0.33. Importantly, none of the analysed

418 sites was from ecological margins of species distribution, which are often considered as  
419 optimal for dendroclimatic investigations. In previous studies, the VS model has already  
420 shown promising performance on independent verification data, e.g. for *Pinus halepensis*  
421 from Tunisia ( $r = 0.63$ ) (Touchan et al. 2012) and *Pinus sylvestris* from Siberia ( $r = 0.53$ )  
422 (Tychkov et al. 2019). The results from VS-Lite are usually less significant. Tumajer et al. (2017)  
423 reported a mean correlation of 0.24 (*Picea abies*), while Breitenmoser et al. (2014) reported  
424 a mean value of 0.29 for the 2287 tree-ring chronologies from the ITRDB network.

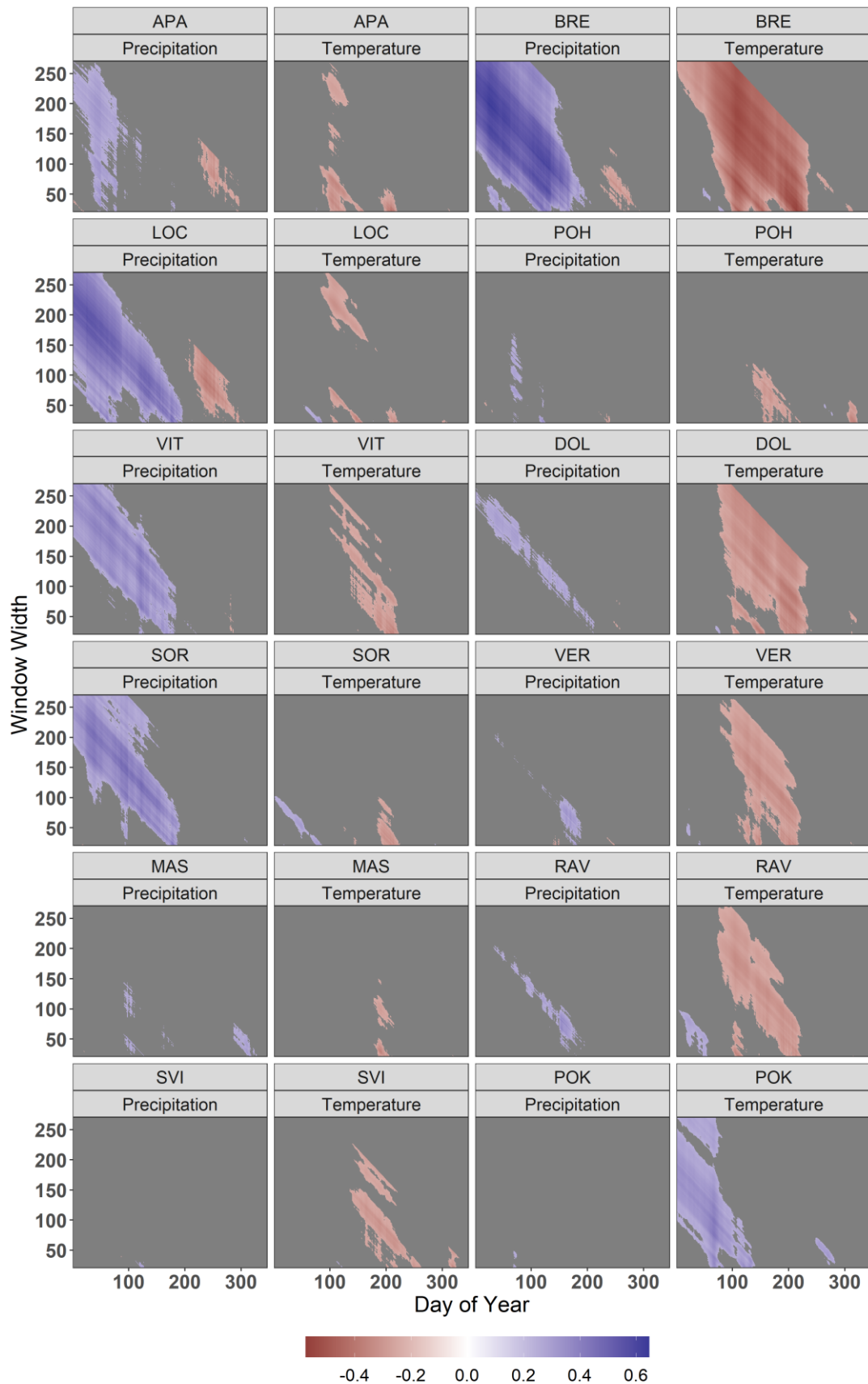
425 We obtained better VS results for dry sites, mostly at low elevations. For instance, sites BRE  
426 and LOC showed very good model performance: In addition to high correlation coefficients  
427 for calibration and verification data, the model realistically simulated the variance, which  
428 resulted in very low error terms (Table 3). For some other sites, e.g. VER and SOR, the model  
429 produced good correlation results, but the variance of simulated chronologies was lower than  
430 the actual one. It must be noted here that parameterization was primarily guided to achieve  
431 high correlation results, rather than low RMSE and bias. The least precise results in our study  
432 were obtained for site SVI. This is not surprising given the concave shape of the local  
433 topography (i.e. typical karst depression). This is also characterised as a cold air pool, which  
434 is associated with local climate conditions and most likely not integrated in gridded climate  
435 products.

436 For some sites, differences in the correlation coefficient between calibration and verification  
437 data were greater, e.g. site DOL (from 0.56 to 0.41) and VIT (from 0.64 to 0.45). We further  
438 explored the possible underlying drivers of this pattern by comparing the performance of the  
439 VS model and associated rbars (Supplementary Figure 5). In general, a drop in the correlation  
440 was associated with a drop in the rbar. A possible explanation of this phenomenon is through  
441 common causality on rbar and VS performance – due to stronger climatic control on tree

442 growth, tree-ring width series of individual trees (Ponocná et al. 2018) and forest site  
443 chronologies (Shestakova et al. 2016) become more tightly synchronized, resulting in  
444 increasing  $r_{bar}$ . At the same time, because of the purely climate-driven algorithm, the VS  
445 model performs best in climatically strongly controlled sites and periods, where climate is the  
446 prevailing driver of tree growth. However, there were some exceptions to the  $r_{bar}$  and  
447 correlation synchronicity, i.e. site VIT, where  $r_{bar}$  was stable, while correlation was  
448 importantly lower for the verification split. It must be noted that different combinations of  
449 parameter values can potentially result in good calibration statistics and that the selected  
450 combination might not be optimal for the entire period in such cases.

451 The VS model has proven to be a reliable tool for modelling radial tree growth as a function  
452 of climate, where fixed environmental influence is defined by properly tuned parameters.  
453 However, in its current form, it seems that approximately 50 % of the explained variance is  
454 the maximum that can be achieved. In addition to the beforementioned consideration of  
455 carry-over effects, a key to achieve even better performance might be related to other known  
456 environmental factors that importantly contribute to radial tree growth and vary from year  
457 to year, such as nitrogen deposition and atmospheric carbon dioxide concentration (Kahle et  
458 al. 2008).





459

460 **Figure 5:** Bootstrapped partial correlation coefficients calculated from day-wise aggregated climate  
 461 temperature and precipitation data of variable widths. The reference position for each value is the  
 462 beginning of the considered window. Only significant correlations with  $p < 0.05$  are shown.

463 **5. CONCLUSIONS**

464 For the majority of European sites, environmental changes will likely lead to less favourable  
465 growth conditions for Norway spruce due to its drought intolerance (Lévesque et al. 2013;  
466 Zweifel et al. 2009; Schuster and Oberhuber 2013; Vitali et al. 2017; Boden et al. 2014).  
467 Representative concentration pathway (RCP) scenarios for Slovenia predict a temperature  
468 rise by 2100 of approximately 1.3 °C (RCP2.6), 2 °C (RCP4.5) and 4.1 °C (RCP8.5). In contrast  
469 to temperature, projections of changes in precipitation are less reliable (e.g. Piniewski et al.  
470 2017; Orth et al. 2016). In the case of the moderately optimistic scenario RCP4.5, no  
471 significant changes are expected initially, while by 2100 the annual mean precipitation  
472 amount is expected to increase by 10 % (summarised by Slovenian Environment Agency  
473 2019). In addition to climate, the future growth of Norway spruce will largely depend on  
474 natural hazards, such as windstorms and insect outbreaks (de Groot and Ogris 2019). Indeed,  
475 a full understanding of climate change-disturbance-forest productivity interactions cannot be  
476 reached because such events may completely change future productivity projections, i.e. an  
477 estimated increase in productivity may be counterbalanced by increased risk of damage due  
478 to extreme weather events.

479 We showed that the climate-related growth of Norway spruce is mainly determined by  
480 summer temperatures (negatively) and spring precipitation (positively). The exception here  
481 are high-elevation sites with annual precipitation sums close to 1900 mm, which are positively  
482 related to higher temperature at the beginning of growing season. Recent trends of radial  
483 growth at analysed sites support such predictions (Supplementary Figure 4). Most of the  
484 temperature limited sites which exhibited negative correlations with summer temperature  
485 showed slight negative trends, i.e. VER, SVI, MAS, RAV, while site POK (positive correlations  
486 with higher summer temperature) exhibited a positive trend in radial tree-growth. For mostly

487 precipitation limited sites, i.e. SOR, POH, VIT, DOL and LOC, a slightly increasing or neutral  
488 trend was shown. Sites BRE and APA have exhibited positive and negative growth trends since  
489 1950, which could be attributed to the interaction of a positive precipitation and negative  
490 temperature effect in the studied period. Based on the climate projections for Slovenia (see  
491 above), the only site that would most likely benefit from such scenarios is site POK. For all  
492 other sites, future radial growth will largely depend on interactions between spring  
493 precipitation and summer temperature and how the projected increase in annual  
494 precipitation will compensate for the projected increase in summer temperature. Longer  
495 growing seasons could partly buffer against the negative effect of increasing temperature,  
496 where growth rates will decline due to higher drought stress in summer, but, simultaneously,  
497 the growing season will start earlier and end later due to increasing spring and autumn  
498 temperatures (Figure 4). Consequently, the decline in total ring width might be less intensive.

499

500 **Acknowledgements:** We are grateful to Samo Stopar and Robert Krajnc, who helped with  
501 the fieldwork and tree-ring processing. We acknowledge the E-OBS dataset from the EU-FP6  
502 project UERRA (<http://www.uerra.eu>) and the Copernicus Climate Change Service, and the  
503 data providers in the ECA&D project (<https://www.ecad.eu>).

504

505 **Funding:** This research was supported by the Slovenian Research Agency: 1) Bilateral  
506 Cooperation between the Slovenian Forestry Institute and Siberian Federal University (ARRS  
507 BI-RU/19-20-016); 2) Target research project “Adaptive management in spruce forests in  
508 Slovenia” (V4-1614) and 3) Program and Research Group “Forest biology, ecology and  
509 technology” (P4-0107). In addition, JT was supported by the Alexander von Humboldt

510 Research Fellowship. VS, MP, and IT were supported by the Russian Ministry of Science and  
511 Higher Education (projects #FSRZ-2020-0010 and #FSRZ-2020-0014).

512

513 **Conflict of interests/Competing interests:** There are no conflict of interests or competing  
514 interests.

515

516 **Availability of data and material:** Tree-ring data is available on request.

517

518 **Code availability:** R code used for the analysis is available upon request from the first author.

519

520 **Author contribution statement:** J.J analysed the data and prepared the first version of the  
521 manuscript; V.S., J.G. and T.L. supervised the study; I.T. and J.T. parameterised the VS model  
522 for all sites; T.L. designed the sampling scheme and collected tree-ring data; J.T. contributed  
523 to the discussion and improved the manuscript; and D.A, P.P and M.P commented on the  
524 manuscript.

525

## 526 **6. REFERENCES**

- 527 Adhikary SK, Muttill N, Yilmaz AG (2017) Cokriging for enhanced spatial interpolation of rainfall in two  
528 Australian catchments. *Hydrological Processes* 31 (12):2143-2161. doi:10.1002/hyp.11163
- 529 Anchukaitis KJ, Evans MN, Hughes MK, Vaganov EA (2020) An interpreted language implementation  
530 of the Vaganov–Shashkin tree-ring proxy system model. *Dendrochronologia* 60:125677.  
531 doi:<https://doi.org/10.1016/j.dendro.2020.125677>
- 532 Andreassen K, Solberg S, Tveito OE, Lystad SL (2006) Regional differences in climatic responses of  
533 Norway spruce (*Picea abies* L. Karst) growth in Norway. *For Ecol Manage* 222 (1):211-221.  
534 doi:<https://doi.org/10.1016/j.foreco.2005.10.029>

- 535 Apaydin H, Sonmez FK, Yildirim YE (2004) Spatial interpolation techniques for climate data in the  
536 GAP region in Turkey. *Clim Res* 28 (1):31-40
- 537 BMEL (2015) The Forests in Germany: Selected Results of the Third National Forest Inventory.  
538 Federal Ministry of Food and Agriculture, Berlin
- 539 BMLFUW (2017) Sustainable forest management in Austria: Key indicators 2017. Federal Ministry of  
540 Agriculture, Forestry, Environment and Water Management, Vienna
- 541 Boden S, Kahle H-P, Wilpert Kv, Spiecker H (2014) Resilience of Norway spruce (*Picea abies* (L.) Karst)  
542 growth to changing climatic conditions in Southwest Germany. *For Ecol Manage* 315:12-21.  
543 doi:<https://doi.org/10.1016/j.foreco.2013.12.015>
- 544 Bouriaud O, Popa I (2009) Comparative dendroclimatic study of Scots pine, Norway spruce, and  
545 silver fir in the Vrancea Range, Eastern Carpathian Mountains. *Trees* 23 (1):95-106.  
546 doi:[10.1007/s00468-008-0258-z](https://doi.org/10.1007/s00468-008-0258-z)
- 547 Breitenmoser P, Brönnimann S, Frank D (2014) Forward modelling of tree-ring width and comparison  
548 with a global network of tree-ring chronologies. *Clim Past* 10 (2):437-449. doi:[10.5194/cp-](https://doi.org/10.5194/cp-10-437-2014)  
549 [10-437-2014](https://doi.org/10.5194/cp-10-437-2014)
- 550 Brus DJ, Hengeveld GM, Walvoort DJJ, Goedhart PW, Heidema AH, Nabuurs GJ, Gunia K (2012)  
551 Statistical mapping of tree species over Europe. *Eur J For Res* 131 (1):145-157.  
552 doi:[10.1007/s10342-011-0513-5](https://doi.org/10.1007/s10342-011-0513-5)
- 553 Bunn AG (2008) A dendrochronology program library in R (dplR). *Dendrochronologia* 26 (2):115-124.  
554 doi:[10.1016/j.dendro.2008.01.002](https://doi.org/10.1016/j.dendro.2008.01.002)
- 555 Buras A, Menzel A (2019) Projecting Tree Species Composition Changes of European Forests for  
556 2061–2090 Under RCP 4.5 and RCP 8.5 Scenarios. *Frontiers in Plant Science* 9 (1986).  
557 doi:[10.3389/fpls.2018.01986](https://doi.org/10.3389/fpls.2018.01986)
- 558 Buras A, Wilmking M (2015) Correcting the calculation of Gleichläufigkeit. *Dendrochronologia* 34:29-  
559 30. doi:<https://doi.org/10.1016/j.dendro.2015.03.003>
- 560 Buttò V, Shishov V, Tychkov I, Popkova M, He M, Rossi S, Deslauriers A, Morin H (2020) Comparing  
561 the Cell Dynamics of Tree-Ring Formation Observed in Microcores and as Predicted by the  
562 Vaganov–Shashkin Model. *Frontiers in Plant Science* 11 (1268). doi:[10.3389/fpls.2020.01268](https://doi.org/10.3389/fpls.2020.01268)
- 563 Carrer M, Motta R, Nola P (2012) Significant Mean and Extreme Climate Sensitivity of Norway Spruce  
564 and Silver Fir at Mid-Elevation Mesic Sites in the Alps. *PLOS ONE* 7 (11):e50755.  
565 doi:[10.1371/journal.pone.0050755](https://doi.org/10.1371/journal.pone.0050755)
- 566 Caudullo G, Tinner W, de Rigo. D (2016) *Picea abies* in Europe: distribution, habitat, usage and  
567 threats. In: San-Miguel-Ayanz J, de Rigo D, Caudullo G, Houston Durrant T, Mauri A (eds)  
568 European Atlas of Forest Tree Species. Publication Office of the European Union,  
569 Luxembourg, pp 114-116
- 570 Cienciala E, Altman J, Doležal J, Kopáček J, Štěpánek P, Stáhl G, Tumajer J (2018) Increased spruce  
571 tree growth in Central Europe since 1960s. *Sci Total Environ* 619-620:1637-1647.  
572 doi:<https://doi.org/10.1016/j.scitotenv.2017.10.138>
- 573 Cornes RC, van der Schrier G, van den Besselaar EJM, Jones PD (2018) An Ensemble Version of the E-  
574 OBS Temperature and Precipitation Data Sets. *Geophys Res Lett: Atmospheres* 123  
575 (17):9391-9409. doi:[10.1029/2017jd028200](https://doi.org/10.1029/2017jd028200)
- 576 de Groot M, Ogris N (2019) Short-term forecasting of bark beetle outbreaks on two economically  
577 important conifer tree species. *For Ecol Manage* 450:117495.  
578 doi:<https://doi.org/10.1016/j.foreco.2019.117495>
- 579 Eckstein D, Bauch J (1969) Beitrag zur Rationalisierung eines dendrochronologischen Verfahrens und  
580 zur Analyse seiner Aussagesicherheit. *Forstwissenschaftliches Zentralblatt* 88:230–250

- 581 Evans MN, Reichert BK, Kaplan A, Anchukaitis KJ, Vaganov EA, Hughes MK, Cane MA (2006) A  
582 forward modeling approach to paleoclimatic interpretation of tree-ring data. *J Geophys Res-*  
583 *Biogeo* 111:G03008. doi:10.1029/2006jg000166
- 584 Furze ME, Huggett BA, Aubrecht DM, Stolz CD, Carbone MS, Richardson AD (2019) Whole-tree  
585 nonstructural carbohydrate storage and seasonal dynamics in five temperate species. *New*  
586 *Phytol* 221 (3):1466-1477. doi:10.1111/nph.15462
- 587 Gričar J, Prislan P, Gryc V, Vavřík H, de Luis M, Čufar K (2014) Plastic and locally adapted phenology  
588 in cambial seasonality and production of xylem and phloem cells in *Picea abies* from  
589 temperate environments. *Tree Physiol* 34 (8):869-881. doi:10.1093/treephys/tpu026
- 590 Guiot J, Boucher E, Gea-Izquierdo G (2014) Process models and model-data fusion in dendroecology.  
591 *Frontiers in Ecology and Evolution* 2 (52). doi:10.3389/fevo.2014.00052
- 592 Hanewinkel M, Cullmann DA, Schelhaas M-J, Nabuurs G-J, Zimmermann NE (2013) Climate change  
593 may cause severe loss in the economic value of European forest land. *Nature Climate*  
594 *Change* 3 (3):203-207. doi:10.1038/nclimate1687
- 595 Hartl-Meier C, Zang C, Dittmar C, Esper J, GÅfÅttlein A, Rothe A (2014) Vulnerability of Norway  
596 spruce to climate change in mountain forests of the European Alps. *Clim Res* 60 (2):119-132
- 597 He M, Shishov V, Kaparova N, Yang B, Bräuning A, Grießinger J (2017a) Process-based modeling of  
598 tree-ring formation and its relationships with climate on the Tibetan Plateau.  
599 *Dendrochronologia* 42:31-41. doi:https://doi.org/10.1016/j.dendro.2017.01.002
- 600 He M, Yang B, Shishov V, Rossi S, Bräuning A, Ljungqvist F, Grießinger J (2018) Relationships between  
601 Wood Formation and Cambium Phenology on the Tibetan Plateau during 1960–2014.  
602 *Forests* 9 (2):86
- 603 He M, Yang B, Shishov V, Rossi S, Bräuning A, Ljungqvist FC, Grießinger J (2017b) Projections for the  
604 changes in growing season length of tree-ring formation on the Tibetan Plateau based on  
605 CMIP5 model simulations. *International Journal of Biometeorology* 62 (4):631–641.  
606 doi:https://doi.org/10.1007/s00484-017-1472-4
- 607 Jevšenak J (2020) New features in the dendroTools R package: Bootstrapped and partial correlation  
608 coefficients for monthly and daily climate data. *Dendrochronologia* 63:125753.  
609 doi:https://doi.org/10.1016/j.dendro.2020.125753
- 610 Jevšenak J, Levanič T (2018) *dendroTools*: R package for studying linear and nonlinear responses  
611 between tree-rings and daily environmental data. *Dendrochronologia* 48:32–39.  
612 doi:10.1016/j.dendro.2018.01.005
- 613 Kahle H-P, Karjalainen T, Schuck A, Ågren GI, Kellomäki S, Mellert KH, Prietzel J, Rehfuss K, Spiecker  
614 H (2008) Causes and Consequences of Forest Growth Trends in Europe – Results of the  
615 RECOGNITION Project, vol 21. European Forest Institute Research Reports. Brill,
- 616 Klimo E, Hager H, Kulhavy J Spruce Monocultures in Central Europe: Problems and Prospects. In,  
617 01/01 2000. European Forest Institute,
- 618 Klopčič M, Mina M, Bugmann H, Bončina A (2017) The prospects of silver fir (*Abies alba* Mill.) and  
619 Norway spruce (*Picea abies* (L.) Karst) in mixed mountain forests under various management  
620 strategies, climate change and high browsing pressure. *Eur J For Res* 136 (5):1071-1090.  
621 doi:10.1007/s10342-017-1052-5
- 622 Kolář T, Čermák P, Trnka M, Žid T, Rybníček M (2017) Temporal changes in the climate sensitivity of  
623 Norway spruce and European beech along an elevation gradient in Central Europe. *Agric For*  
624 *Meteorol* 239:24-33. doi:https://doi.org/10.1016/j.agrformet.2017.02.028
- 625 Koprowski M, Zielski A (2006) Dendrochronology of Norway spruce (*Picea abies* (L.) Karst.) from two  
626 range centres in lowland Poland. *Trees* 20 (3):383. doi:10.1007/s00468-006-0051-9

- 627 Levanič T (2007) ATRICS - A new system for image acquisition in dendrochronology. *Tree-Ring Res* 63  
628 (2):117–122. doi:10.3959/1536-1098-63.2.117
- 629 Levanič T, Gričar J, Gagen M, Jalkanen R, Loader NJ, McCarroll D, Oven P, Robertson I (2008) The  
630 climate sensitivity of Norway spruce [*Picea abies* (L.) Karst.] in the southeastern European  
631 Alps. *Trees* 23 (1):169. doi:10.1007/s00468-008-0265-0
- 632 Lévesque M, Saurer M, Siegwolf R, Eilmann B, Brang P, Bugmann H, Rigling A (2013) Drought  
633 response of five conifer species under contrasting water availability suggests high  
634 vulnerability of Norway spruce and European larch. *Global Change Biol* 19 (10):3184-3199.  
635 doi:10.1111/gcb.12268
- 636 Linderholm HW (2006) Growing season changes in the last century. *Agric For Meteorol* 137 (1):1-14.  
637 doi:https://doi.org/10.1016/j.agrformet.2006.03.006
- 638 Linderholm HW, Walther A, Chen D (2008) Twentieth-century trends in the thermal growing season  
639 in the Greater Baltic Area. *Clim Change* 87 (3):405-419. doi:10.1007/s10584-007-9327-3
- 640 Mäkinen H, Nöjd P, Mielikäinen K (2000) Climatic signal in annual growth variation of Norway spruce  
641 (*Picea abies*) along a transect from central Finland to the Arctic timberline. *Can J For Res* 30  
642 (5):769-777. doi:10.1139/x00-005
- 643 Menzel A, Fabian P (1999) Growing season extended in Europe. *Nature* 397 (6721):659-659.  
644 doi:10.1038/17709
- 645 MPSR (2019) Správa o lesnom hospodárstve v Slovenskej republike za rok 2018 (in Slovak language).  
646 Ministry of Agriculture and Rural Development of the Slovak Republic, Bratislava
- 647 MZe (2018) Zpráva o stavu lesa a lesního hospodářství České republiky v roce 2018 (in Czech  
648 language). Ministry of Agriculture of the Czech Republic, Prague
- 649 Orth R, Zscheischler J, Seneviratne SI (2016) Record dry summer in 2015 challenges precipitation  
650 projections in Central Europe. *Scientific Reports* 6 (1):28334. doi:10.1038/srep28334
- 651 Park T, Ganguly S, Tømmervik H, Euskirchen ES, Høgda K-A, Karlsen SR, Brovkin V, Nemani RR,  
652 Myneni RB (2016) Changes in growing season duration and productivity of northern  
653 vegetation inferred from long-term remote sensing data. *Environ Res Lett* 11 (8):084001.  
654 doi:10.1088/1748-9326/11/8/084001
- 655 Piniewski M, Mezghani A, Szcześniak M, Kundzewicz Z (2017) Regional projections of temperature  
656 and precipitation changes: Robustness and uncertainty aspects. *Meteorol Z* 26:223-234
- 657 Ponocná T, Chuman T, Rydval M, Urban G, Migała K, Tremł V (2018) Deviations of treeline Norway  
658 spruce radial growth from summer temperatures in East-Central Europe. *Agric For Meteorol*  
659 253-254:62-70. doi:https://doi.org/10.1016/j.agrformet.2018.02.001
- 660 Ponocná T, Spyt B, Kaczka R, Büntgen U, Tremł V (2016) Growth trends and climate responses of  
661 Norway spruce along elevational gradients in East-Central Europe. *Trees* 30 (5):1633-1646.  
662 doi:10.1007/s00468-016-1396-3
- 663 Popkova MI, Vaganov EA, Shishov VV, Babushkina EA, Rossi S, Fonti MV, Fonti P (2018) Modeled  
664 Tracheidograms Disclose Drought Influence on *Pinus sylvestris* Tree-Rings Structure From  
665 Siberian Forest-Steppe. *Frontiers in Plant Science* 9 (1144). doi:10.3389/fpls.2018.01144
- 666 Pretzsch H, Biber P, Schütze G, Uhl E, Rötzer T (2014) Forest stand growth dynamics in Central  
667 Europe have accelerated since 1870. *Nat Commun* 5:4967-4967. doi:10.1038/ncomms5967
- 668 Rabbel I, Neuwirth B, Bogena H, Diekkrüger B (2018) Exploring the growth response of Norway  
669 spruce (*Picea abies*) along a small-scale gradient of soil water supply. *Dendrochronologia*  
670 52:123-130. doi:https://doi.org/10.1016/j.dendro.2018.10.007
- 671 Reyer CPO, Bathgate S, Blennow K, Borges JG, Bugmann H, Delzon S, Faias SP, Garcia-Gonzalo J,  
672 Gardiner B, Gonzalez-Olabarria JR, Gracia C, Hernández JG, Kellomäki S, Kramer K, Lexer MJ,

- 673 Lindner M, van der Maaten E, Maroschek M, Muys B, Nicoll B, Palahi M, Palma JHN, Paulo  
674 JA, Peltola H, Pukkala T, Rammer W, Ray D, Sabaté S, Schelhaas M-J, Seidl R, Temperli C,  
675 Tomé M, Yousefpour R, Zimmermann NE, Hanewinkel M (2017) Are forest disturbances  
676 amplifying or canceling out climate change-induced productivity changes in European  
677 forests? *Environ Res Lett* 12 (3):034027. doi:10.1088/1748-9326/aa5ef1
- 678 Rossi S, Deslauriers A, Gričar J, Seo J-W, Rathgeber CB, Anfodillo T, Morin H, Levanic T, Oven P,  
679 Jalkanen R (2008) Critical temperatures for xylogenesis in conifers of cold climates. *Global  
680 Ecol Biogeogr* 17 (6):696-707. doi:10.1111/j.1466-8238.2008.00417.x
- 681 Schelhaas M-J, Nabuurs G-J, Schuck A (2003) Natural disturbances in the European forests in the  
682 19th and 20th centuries. *Global Change Biol* 9 (11):1620-1633. doi:10.1046/j.1365-  
683 2486.2003.00684.x
- 684 Schuster R, Oberhuber W (2013) Drought sensitivity of three co-occurring conifers within a dry inner  
685 Alpine environment. *Trees (Berlin, Germany : West)* 27 (1):61-69. doi:10.1007/s00468-012-  
686 0768-6
- 687 Seidl R, Müller J, Hothorn T, Bässler C, Heurich M, Kautz M (2016) Small beetle, large-scale drivers:  
688 how regional and landscape factors affect outbreaks of the European spruce bark beetle. *J  
689 Appl Ecol* 53 (2):530-540. doi:10.1111/1365-2664.12540
- 690 Shestakova TA, Gutiérrez E, Kirilyanov AV, Camarero JJ, Génova M, Knorre AA, Linares JC, Resco de  
691 Dios V, Sánchez-Salguero R, Voltas J (2016) Forests synchronize their growth in contrasting  
692 Eurasian regions in response to climate warming. *Proc Natl Acad Sci USA*:201514717.  
693 doi:10.1073/pnas.1514717113
- 694 Shishov VV, Tychkov II, Popkova MI, Ilyin VA, Bryukhanova MV, Kirilyanov AV (2016) VS-oscilloscope:  
695 A new tool to parameterize tree radial growth based on climate conditions.  
696 *Dendrochronologia* 39:42-50. doi:https://doi.org/10.1016/j.dendro.2015.10.001
- 697 Sidor CG, Popa I, Vlad R, Cherubini P (2015) Different tree-ring responses of Norway spruce to air  
698 temperature across an altitudinal gradient in the Eastern Carpathians (Romania). *Trees* 29  
699 (4):985-997. doi:10.1007/s00468-015-1178-3
- 700 Skudnik M, Grah A, Poljanec A Changes in the structure and tree composition of Slovenian forests in  
701 the last ten years. In: Kraigher H, Humar M (eds) *Climate change and forest*, Ljubljana, 2019.  
702 *Silva Slovenica*, pp 2-7
- 703 Slovenian Environment Agency (2019) *Climate change projections for Slovenia over the 21st century:  
704 Temperature and precipitation summary*. Ministry of the Environment and Spatial Planning,  
705 Ljubljana
- 706 Spiecker H (2003) Silvicultural management in maintaining biodiversity and resistance of forests in  
707 Europe—temperate zone. *J Environ Manage* 67 (1):55-65.  
708 doi:https://doi.org/10.1016/S0301-4797(02)00188-3
- 709 St. George S, Meko DM, Evans MN (2008) Regional tree growth and inferred summer climate in the  
710 Winnipeg River basin, Canada, since AD 1783. *Quatern Res* 70 (2):158-172.  
711 doi:https://doi.org/10.1016/j.yqres.2008.04.009
- 712 Tērauds A, Brūmelis G, Nikodemus O (2011) Seventy-year changes in tree species composition and  
713 tree ages in state-owned forests in Latvia. *Scand J For Res* 26 (5):446-456.  
714 doi:10.1080/02827581.2011.586647
- 715 Tolwinski-Ward SE, Evans MN, Hughes MK, Anchukaitis KJ (2011) An efficient forward model of the  
716 climate controls on interannual variation in tree-ring width. *Clim Dynam* 36 (11-  
717 12):2419–2439. doi:10.1007/s00382-010-0945-5



- 718 Touchan R, Shishov VV, Meko DM, Nouiri I, Grachev A (2012) Process based model sheds light on  
719 climate sensitivity of Mediterranean tree-ring width. *Biogeosciences* 9 (3):965-972.  
720 doi:10.5194/bg-9-965-2012
- 721 Touchan R, Shishov VV, Tychkov II, Sivrikaya F, Attieh J, Ketmen M, Stephan J, Mitsopoulos I, Christou  
722 A, Meko DM (2016) Elevation-layered dendroclimatic signal in eastern Mediterranean tree  
723 rings. *Environ Res Lett* 11 (4):044020. doi:10.1088/1748-9326/11/4/044020
- 724 Tumajer J, Altman J, Štěpánek P, Tremli V, Doležal J, Cienciala E (2017) Increasing moisture limitation  
725 of Norway spruce in Central Europe revealed by forward modelling of tree growth in tree-  
726 ring network. *Agric For Meteorol* 247:56-64.  
727 doi:https://doi.org/10.1016/j.agrformet.2017.07.015
- 728 Tychkov II, Sviderskaya IV, Babushkina EA, Popkova MI, Vaganov EA, Shishov VV (2019) How can the  
729 parameterization of a process-based model help us understand real tree-ring growth? *Trees*  
730 33 (2):345-357. doi:10.1007/s00468-018-1780-2
- 731 Vaganov EA, Hughes MK, Shashkin AV (2006) *Growth Dynamics of Conifer Tree Rings : Images of Past  
732 and Future Environments. Ecological studies,, vol 183. Springer, Berlin*
- 733 Valinger E, Kempe G, Fridman J (2014) Forest management and forest state in southern Sweden  
734 before and after the impact of storm Gudrun in the winter of 2005. *Scand J For Res* 29  
735 (5):466-472. doi:10.1080/02827581.2014.927528
- 736 van der Maaten-Theunissen M, Kahle H-P, van der Maaten E (2013) Drought sensitivity of Norway  
737 spruce is higher than that of silver fir along an altitudinal gradient in southwestern Germany.  
738 *Annals of Forest Science* 70 (2):185-193. doi:10.1007/s13595-012-0241-0
- 739 Vitali V, Büntgen U, Bauhus J (2017) Silver fir and Douglas fir are more tolerant to extreme droughts  
740 than Norway spruce in south-western Germany. *Global Change Biol* 23 (12):5108-5119.  
741 doi:10.1111/gcb.13774
- 742 Zweifel R, Rigling A, Dobbertin M (2009) Species-specific stomatal response of trees to drought – a  
743 link to vegetation dynamics? *Journal of Vegetation Science* 20 (3):442-454.  
744 doi:10.1111/j.1654-1103.2009.05701.x